

Integrative nucleophosmin mutation-associated microRNA and gene expression pattern analysis identifies novel microRNA - target gene interactions in acute myeloid leukemia

Annika C. Russ,¹ Sandrine Sander,² Sonja C. Lück,¹ Katharina M. Lang,¹ Marion Bauer,¹ Frank G. Rücker,¹ Hans A. Kestler,³ Richard F. Schlenk,¹ Hartmut Döhner,¹ Karlheinz Holzmann,⁴ Konstanze Döhner,¹ and Lars Bullinger¹

¹Department of Internal Medicine III, University Hospital Ulm; ²Institute of Physiological Chemistry, University of Ulm; ³Institute of Neural Information Processing, University of Ulm; and ⁴Microarray Core Facility, University of Ulm, Germany

Citation: Russ AC, Sander S, Lück SC, Lang KM, Bauer M, Rücker FG, Kestler HA, Schlenk RF, Döhner H, Holzmann K, Döhner K, and Bullinger L. Integrative nucleophosmin mutation-associated microRNA and gene expression pattern analysis identifies novel microRNA - target gene interactions in acute myeloid leukemia. *Haematologica* 2011;96(12):1783-1791. doi:10.3324/haematol.2011.046888

Supplementary Design and Methods

Patients' samples

Samples from 43 adult patients (median age 46 years; range, 23-60) with cytogenetically normal acute myeloid leukemia (CN-AML) were provided by the German-Austrian AML Study Group (AML SG) with informed consent of the patients and institutional review board approval from all participating centers. Samples were enriched for mononuclear cells by Ficoll gradient purification from diagnostic (i.e. pre-treatment) peripheral blood (n=24) or bone marrow (n=19) samples. Following enrichment, the percentage of leukemic cells was at least 80%. All patients were enrolled into the AML SG treatment protocol AML HD98A (ClinicalTrials.gov Identifier: NCT00146120). Twenty-three of the 43 patients (53%) had mutated *NPM1*. Details of the clinical characteristics of patients, as well as the results of molecular genetic analyses are provided in *Online Supplementary Table S1*.

Cytogenetic and molecular genetic analyses

Conventional cytogenetic (chromosome banding), interphase cytogenetic (fluorescence *in situ* hybridization, FISH), and molecular genetic analyses [screening for *FLT3* internal tandem-duplications (ITD) and tyrosine kinase domain (TKD) mutations, *CEPBA* mutations and *NPM1* mutations (*NPM1^{mut}*)] were performed as previously described at the central reference laboratory of the AML SG at our institution.¹⁻⁵

Cell lines and cell culture

Leukemic cell lines (CMK, HEL, K-562, Kasumi-1, KG-1, M-07e, ME-1, MONO-MAC-1, MV4-11, NB-4, OCI-AML2, OCI-AML5, THP-1, UT-7) and HeLa cells were purchased from the German Collection of Microorganisms and Cell Cultures (DSMZ) and cultured according to their guidelines (www.dsmz.de/human_and_animal_cell_lines/).

miRNA expression profiling

To screen miRNA expression in AML and leukemic cell lines, we set up a microarray platform using a commercially available oligonucleotide probe set based on version 6.0 of the Sanger miRNA database (*mirVana* miRNA Probe Set, Ambion). In brief, this probe set, representing 281 human miRNAs, was spotted

onto GAPS-coated glass slides (Corning). Total RNA was isolated from frozen mononuclear AML samples and leukemic cell lines using the *mirVana* miRNA Isolation Kit (Ambion). Pooled RNA from nine different tumor cell lines served as a common reference for both miRNA and gene expression analyses (see below).^{6,7} Size-fractionated small RNA (flashPAGE Fractionator System, Ambion) containing only the mature miRNA fraction was labeled for microarray analysis using an end-labeling strategy (*mirVana* miRNA Labeling Kit, Ambion). Following purification, the Cy5-labeled AML and Cy3-labeled common reference samples were mixed, co-hybridized for 14 hours onto the miRNA microarrays and washed according to the manufacturer's protocol (Ambion).

Microarrays were imaged, and log₂ transformed fluorescence ratios were normalized and filtered as previously described.⁷ The complete filtered miRNA microarray dataset is provided as in *Online Supplementary Table S2* (arrays from 3 patients were excluded because of borderline quality). For hierarchical cluster analysis, we applied average linkage clustering (distance measure: correlation uncentered) and visualized results using TreeView (Eisen Lab; <http://rana.lbl.gov/eisen/>).⁸

Validation of microRNA findings

Northern blot analysis and quantitative reverse transcriptase polymerase chain reaction (qRT-PCR) of selected miRNAs using the TaqMan MicroRNA Reverse Transcription Kit and MicroRNA Assays (Applied Biosystems) were performed as previously described,⁹ and as described below.

Northern blot analysis of microRNAs

For technical validation of miRNA microarray findings, we performed northern blot analyses for miR-20a and let-7a. Briefly, 10 µg of total RNA were separated on denaturing polyacrylamide gels and transferred to positively charged nylon membranes. Membranes were incubated with ³²P-labeled probes, complementary to the respective miRNAs, which were designed and processed according to the *mirVana* miRNA probe construction kit (Ambion). Next, the membranes were washed and subjected to autoradiography. As a loading control, total RNA was detected by ethidium bromide staining of the gels before transfer to the membrane.

Quantitative reverse transcriptase polymerase chain reaction for microRNA detection

Microarray based miRNA expression findings were also validated by qRT-PCR of selected miRNAs using the TaqMan MicroRNA Reverse Transcription Kit and MicroRNA Assays (Applied Biosystems) according to the manufacturer's protocols (Applied Biosystems). miR-374 was used for data normalization, as this miRNA, according to our analysis, was expressed at a well detectable level with only slight variation among the samples, and therefore served as an endogenous control. The qPCR analysis was run on a 7900HT Fast Real-Time PCR System (Applied Biosystems).

Gene expression profiling

Gene expression profiling (GEP) had been previously performed on all 43 samples using TRIzol (Invitrogen) prepared RNA from identical pre-treatment samples and cDNA microarrays provided by the Stanford Functional Genomics Facility.^{7,10} The complete gene expression microarray dataset is available at the Gene Expression Omnibus data repository (accession number: GSE31644).

Data analysis of microarray based expression data sets

Supervised analyses were performed on data sets of varying filter criteria stringency. To correlate miRNA and/or mRNA expression findings with molecular genetics, the Significance Analysis of Microarrays (SAM) method with adjustment for multiple testing was used (false discovery rate < 10%).¹¹ Analyses were performed using BRB-Array Tools Version 3.6.1 (developed by Dr. Richard Simon and Amy Peng Lam, available at <http://linus.nci.nih.gov/BRB-ArrayTools.html>) and R Version 2.6.0 (available at www.r-project.org).

Immunoblot analysis

Total cell extracts were fractionated on 12% or 4-12% sodium dodecylsulfate polyacrylamide gels (NuPAGE Bis-Tris Gels, Invitrogen) and electroblotted to polyvinylidene fluoride membranes (Immobilon-P, Millipore). Membranes were reacted with anti-N-Ras (F155, sc-31; Santa Cruz Biotechnology), anti-E2F1 (clones KH20&KH95; Upstate), anti-APP (A 8717; Sigma), anti-cyclin-D1 (H-295, sc-753; Santa Cruz Biotechnology), anti-IRF2 (C-19, sc-498; Santa Cruz Biotechnology), anti-SPARC (H-90, sc-25574; Santa Cruz Biotechnology), anti- β -actin (ab8227; Abcam) or anti- α -tubulin (ab7291; Abcam), followed by incubation with secondary horse radish peroxidase-linked antibodies (GE Healthcare). Immunoreactivity was determined using ECL Western Blotting detection reagents (GE Healthcare). Blots were quantified using ImageJ (available at <http://rsbweb.nih.gov/ij/>).

Luciferase reporter assays

Large parts of the 3'UTR (containing one or two putative miRNA binding sites) or, if less than 1500 bp in length, the full-length 3'UTR of predicted target genes were cloned into the 3'UTR region of the firefly luciferase reporter gene in the pMIR-REPORT vector (Ambion), which was cleaved with SpeI or SpeI/ HindIII. The SpeI restriction site is marked in green. The Hind III restriction site is marked in blue. The 3'UTR was amplified by PCR from cDNA of cell lines using the following primers (all 5' to 3'):

SPARC:

fwd: GCATACTAGTCCTTCCACAGTACCGGATTC

rev: GCATAAGCTTCCGGTGTGTGTGTACAGGTG

CLCN3:

fwd: GCTAACTAGTGAGAGAAGAAACGGAAGAGGA

rev: GCTAACTAGTCAGAATACTTCCTTCTCTTTACTGTCA

CRKL:

fwd: GCATACTAGTCCCTTTACGCACGTCAAAAT

rev: CTGAACTAGTTGGTCTCCCTAGTCACTAAAACA

IRF2:

fwd: GCATACTAGTACTCTCCGCGGTGGTTGT

rev: GCTAACTAGTTCATTTATTATCAATCCACAGGAAAA

KIT:

fwd: GCATACTAGTCTTGATCCAACCTCCAGGAT

rev: GCTAACTAGTTGAAGTGCCCTGAAGTACC

MNI:

fwd: GTCACTAGTTGACAAGAAAGATCCCCTCCT

rev: GCATAAGCTTCGTTTTAGTAAGACACGCTCGTT

SERPIN9:

fwd: GTCACTAGTAATTGCAGTCCAAATCCCATA

rev: GCATAAGCTTTCCTAGATATATACCCAAGAGAATGC

As a control, the predicted miRNA binding sites were mutated by introducing three base pair changes using the QuikChange Lightning site-directed mutagenesis kit (Agilent Technologies Stratagene Products) according to the manufacturer's protocol. Primers were designed using the QuikChange

Primer Design Program on the manufacturer's website (<http://www.genomics.agilent.com/>). For constructs with two predicted miRNA binding sites (BS), BS1 is located closer to the 5' end and BS2 closer to the 3' end of the gene.

The sequences of primers used for site-directed mutagenesis were as follows (the mutated miRNA binding sites are shaded in gray):

SPARC:

miR-29a BS1_sense: 5'-ggtttgtttctcctcctgagacaagtttcgacatagatttaagtgaatacattaac-3'
 miR-29a BS1_antisense: 5'-gttaattgattcaactaaatcatgtcgaactgtctccagcagacaacaacc-3'
 miR-29a BS2_sense: 5'-acatagatttaagtgaatacattacgttcgaaaatgaaattctaacccaagacatgaga-3'
 miR-29a BS2_antisense: 5'-tgcatgttctgggttagaatttcatttcgaaacgtaattgattcaactaaatcatgt-3'

CLCN3:

miR-15a BS1_sense: 5'-tgatatacaagctgtgtgacataaataaaatcgggtgctttgacagtaagaaga-3'
 miR-15a BS1_antisense: 5'-tcttcttactgcaaacgcccgaattttattatgctcaacagcactgtatataca-3'

CRKL:

miR-15a BS1_sense: 5'-gctgttccctcttctcctcgggtttgttctcctgtc-3'
 miR-15a BS1_antisense: 5'-gacagcagacaacaaccggaaggaaacaggcgaacagc-3'
 miR-15a BS2_sense: 5'-tcaggtcggcagagaaggtctcgggtcactactgtctc-3'
 miR-15a BS2_antisense: 5'-gagaccagatgaccgcaaccaatttctcggcagcctga-3'

IRF2:

miR-20a BS1_sense: 5'-tgccttgcaccttatttaaaagagtgacagataggccttctgtg-3'
 miR-20a BS1_antisense: 5'-cacaagaagcctactgtcactcctttaaagataaggtgcagaagca-3'

KIT:

miR-19a BS1_sense: 5'-ggcgttatcggaaagtaaccattgtctctggagttctatgctct-3'
 miR-19a BS1_antisense: 5'-agagcaatgaaactcagagaaactgttactccagataacggcc-3'
 miR-20a BS1_sense: 5'-caatcctgcttctgacactcgtgagtgccgatgattttgca-3'
 miR-20a BS1_antisense: 5'-tgacaanaatcagcggccactcagctgctcagaaagacaggattg-3'

MNI:

miR-15a BS1_sense: 5'-tagatgacctcttctctgtttgttttcaatcgggtgatgccaagtattgta-3'
 miR-15a BS1_antisense: 5'-taacaatacttgacatacaccgaatgaaacaacaagaagaagatcactca-3'
 miR-15a BS2_sense: 5'-agggcagcgaacttggcttgggtgatcctgca-3'
 miR-15a BS2_antisense: 5'-tgcagcatcaccgaaaccaagtgctgcccct-3'

SERPINB9:

miR-29a BS1_sense: 5'-cttaaccctgctcctcagtgtaataaattgggttagatattgactattttataga-3'
 miR-29a BS1_antisense: 5'-tctataaataatgacaaatattcaccattttattaccactgagcagcgggttaag-3'
 miR-29a BS2_sense: 5'-gatattgctactattttatagattccttgggttagctataaaaaggttgaatagtaac-3'
 miR-29a BS2_antisense: 5'-gtacatttacaacctttttatagcctaaccccaaggaaactataaataatgacaaatc-3'

References

- Schlenk RF, Dohner K, Krauter J, Frohling S, Corbacioglu A, Bullinger L, et al. Mutations and treatment outcome in cytogenetically normal acute myeloid leukemia. *N Engl J Med.* 2008; 358(18):1909-18.
- Dohner K, Schlenk RF, Habdank M, Scholl C, Rucker FG, Corbacioglu A, et al. Mutant nucleophosmin (NPM1) predicts favorable prognosis in younger adults with acute myeloid leukemia and normal cytogenetics: interaction with other gene mutations. *Blood.* 2005;106(12):3740-6.
- Frohling S, Schlenk RF, Breittrück J, Benner A, Kreitmeier S, Tobis K, et al. Prognostic significance of activating FLT3 mutations in younger adults (16 to 60 years) with acute myeloid leukemia and normal cytogenetics: a study of the AML Study Group Ulm. *Blood.* 2002;100(13):4372-80.
- Frohling S, Schlenk RF, Stolze I, Bihlmayr J, Benner A, Kreitmeier S, et al. CEBPA mutations in younger adults with acute myeloid leukemia and normal cytogenetics: prognostic relevance and analysis of cooperating mutations. *J Clin Oncol.* 2004;22(4):624-33.
- Frohling S, Schlenk RF, Kayser S, Morhardt M, Benner A, Dohner K, et al. Cytogenetics and age are major determinants of outcome in intensively treated acute myeloid leukemia patients older than 60 years: results from AMLSG trial AML HD98-B. *Blood.* 2006;108(10):3280-8.
- Perou CM, Sorlie T, Eisen MB, van de Rijn M, Jeffrey SS, Rees CA, et al. Molecular portraits of human breast tumours. *Nature.* 2000;406(6797):747-52.
- Bullinger L, Dohner K, Bair E, Frohling S, Schlenk RF, Tibshirani R, et al. Use of gene-expression profiling to identify prognostic sub-classes in adult acute myeloid leukemia. *N Engl J Med.* 2004;350(16):1605-16.
- Eisen MB, Spellman PT, Brown PO, Botstein D. Cluster analysis and display of genome-wide expression patterns. *Proc Natl Acad Sci USA.* 1998;95(25):14863-8.
- Sander S, Bullinger L, Klapproth K, Fiedler K, Kestler HA, Barth TF, et al. MYC stimulates EZH2 expression by repression of its negative regulator miR-26a. *Blood.* 2008;112(10):4202-12.
- Kharas MG, Lengner CJ, Al-Shahrour F, Bullinger L, Ball B, Zaidi S, et al. Musashi-2 regulates normal hematopoiesis and promotes aggressive myeloid leukemia. *Nat Med.* 2010; 16(8):903-8.
- Tusher VG, Tibshirani R, Chu G. Significance analysis of microarrays applied to the ionizing radiation response. *Proc Natl Acad Sci USA.* 2001;98(9):5116-21.

For the reporter assays, HeLa cells were cultured in 24-well plates and transfected with a firefly luciferase-reporter construct (with wild-type or mutated miRNA binding sites), plus a renilla containing vector (CMV-Renilla) in a ratio of 6:1, using Lipofectamine 2000 transfection reagent (Invitrogen; 300 ng DNA, 0.9 µL LF2000 per well). Cells were co-transfected with either a Pre-miR or a negative control RNA (Ambion) at a final concentration of 50 nM. Firefly and renilla luciferase activities were measured 30-38 h after transfection using the Dual-Luciferase Reporter Assay System (Promega).

Nucleofection of myeloid cell lines

For target gene investigations and functional analyses, HEL and K-562 cells were transfected with Pre-miRs at a final concentration of 100 nM using the Nucleofector II Device and Cell Line Nucleofector Kit V (Lonza). For both HEL and K-562 cells, 2x10⁶ cells per nucleofection were used (volume per well: 2.1 mL; HEL: nucleofector program X-005; K-562: program T-016).

Transfection efficiencies, monitored by green fluorescent protein (GFP) plasmid transfection, were as follows:

HEL, 48 h post-transfection	% viable cells	% GFP positive cells in viable cells	% GFP positive cells in total cells
Non-transfected cells	84%	0%	0%
GFP-transfected cells	66%	89%	58%

K-562, 48 h post-transfection	% viable cells	% GFP positive cells in viable cells	% GFP positive cells in total cells
Non-transfected cells	87%	0%	0%
GFP-transfected cells	80%	86%	68%

Online Supplementary Table S1. Clinicopathological characteristics of sample sets.

Clinicopathological parameter		CN-AML samples (n=43)
Sex	Male	n=21/43 (49%)
	Female	n=22/43 (51%)
Age (in years)	Median (range)	46 (23-60)
White blood cell count (x10 ⁹ /L)	Median (range)	46 (2-192)
Lactate dehydrogenase (in U/L)	Median (range)	559 (139-2800)
Preceding malignancy		n=0/43 (0%)
French-American-British classification	FAB M0	n=3/43 (7%)
	FAB M1	n=13/43 (30%)
	FAB M2	n=8/43 (19%)
	FAB M3	n=0/43 (0%)
	FAB M4	n=13/43 (30%)
	FAB M5	n=6/43 (14%)
	FAB M6	n=0/43 (0%)
Molecular markers	<i>FLT3</i> -ITD mutation	n=19/43 (44%)
	<i>FLT3</i> -TKD mutation	n=8/43 (19%)
	<i>NPM1</i> mutation	n=23/43 (53%)
	<i>CEBPA</i> mutation	n=6/40 (15%)
Follow-up (days)	Median (range)	
	All patients	322 (19-2780)
	Survivors	1654 (1033-2780)
Deaths		n=31/43 (72%)

Online Supplementary Table S2. See attached Excel file: ARuss_SupplemTableS2
Data have been normalized and log₂ transformed.

Online Supplementary Table S3. Quantitative RT-PCR for mRNA detection: primer sequences and cycling program.

Primer sequences:		
gene name		Sequence (5' to 3')
Predicted target genes:		
ABCC5	fwd	AGAACTCGACCGTTGGAATGC
	rev	CATGATGGTACTTTCCCTTGGG
AKAP13	fwd	GCCCGCGAGAGACATTGAT
	rev	TTCTCCTCGGTTAGAAGCTGG
APP	fwd	CATCCCCACTTTGTGATTCC
	rev	GTTTCGCAACATCCATCCT
BCL2L1	fwd	CATGGCAGCAGTAAAGCAAG
	rev	TGCTGCATTGTTCCCATAGA
CCND1	fwd	GAACAAACAGATCATCCGCAAC
	rev	GCGGTAGTAGGACAGGAAGTTG
CLCN3	fwd	GCATAGACGGATCAACAGCA
	rev	TGGTGTACCACAACGCACT
CRKL	fwd	CCAGGAATTTGACCAATTGC
	rev	ATTGGTGGGCTTGGATACCT
DUSP16	fwd	TGACTTTATCCCCGAGTCTCAT
	rev	GAGATCCAGCTAAACAGTGC
FOXA1	fwd	GAAGATGGAAGGGCATGAAA
	rev	CGCTCGTAGTCATGGTGTTC
FOXO1	fwd	AAGAGCGTGCCCTACTTCAA
	rev	TTCTTCAITTCGCACACGA
FOXO3	fwd	CTTCAAGGATAAGGGCGACA
	rev	TCTTGCCAGTTCCCTCATTC
FOXO4	fwd	TTGCCAGATCTACGAGTGG
	rev	TCGAGTTCCTCCATCCTGCT
GAB1	fwd	ACTACCTGTTGCTCATCACTG
	rev	GGGACGTTATCATGGAGTCTG
GSPT1	fwd	GGCAAAGACAGCAGGTGTAAG
	rev	GCTCCAGTAAGTCCCTGAGCAG
ID2	fwd	CTGGACTCGCATCCCACTAT
	rev	AATTCAGAAGCCTGCAAGGA
IRF2	fwd	CTACCGAATGCTGCCCTATC
	rev	CCAGAGATGACTCAACTGGTTC
ITGA6	fwd	GTTGCTGTTGGTTCCCTCTC
	rev	TGGAGGCATATCCCACTAGG
KAT2B	fwd	CGAATCGCCGTGAAGAAAAGC
	rev	GAGGGGTTAGGGTTTTCCAG
KIT	fwd	GTTCTGCTCCTACTGCTTCGC
	rev	CCACGCGGACTATTAAGTCTGA
LPP	fwd	AACCCAGCATTTCAGTGTC
	rev	ACCCTCACCTCCAGTTGTT
LRP6	fwd	GAGTTGGATCAACCCAGAGC
	rev	CGACTTGAACCATCCATTCC
MAP4K4	fwd	AAGAACCACACTCTATGATCCA
	rev	GCTACTGATGTAGGCATCTCTCC
MLL	fwd	TCTGTACGTTTGTGGAAGG
	rev	CTTTGCCTGGAGTTGTGGAT
MN1	fwd	GAGCACCATTGACCTGGACT
	rev	GGATGCTGAGGCCTTGTTT
MXI1	fwd	GCCAAAGCACATCAAGAA
	rev	ACCCTGCAGCTGTTCCAGT
NRP1	fwd	CAAGATCGACGTTAGCTCCA
	rev	AACATCTGTGGGGTTGGTGT
OTX2	fwd	AAGCACTGTTTGGCAAGACC
	rev	CATACTGCACCCCTCGACTC
PAWR	fwd	AAGCACAACCAAGTGTCTGAA
	rev	CTGAAACAATTTGCATCCCTGT
PIK3CA	fwd	CCCAGGTGGAATGAATGGCT
	rev	AGCACCCCTTCGGCCCTTAAC

PRKCE	fwd	GGAAAAAGCTCAITTGCTGGT
	rev	AGGTGGGTGCTGACTTGGAT
PROM1	fwd	GCAATCTCCCTGTTGGTGAT
	rev	CCAGTTTCCGACTCCTTTTG
RALA	fwd	AAGTCATCATGGTGGGCAGT
	rev	AGTCTCCACAAAATCATCG
SERPIN9	fwd	TCAACACCTGGGTCTCAAAA
	rev	CATCATCTGCAGTGGCCTTT
SIRT1	fwd	CAGCATCTTGCTGATTTGT
	rev	CATCGAGGAACCTACCTGATTA
SP100	fwd	GGACAAGACCAGACTTTTCA
	rev	TAGGAGCCTTCTACCATGC
SP140	fwd	AACTTCAGGATGGTGCAGAG
	rev	TGGCCTTGTATTGCACTTGC
SPARC	fwd	GGGCCTTGCAATATACCC
	rev	TACAGGGTGACCAGGACGTT
TAL1	fwd	AGCCGGATGCCTTCCCTAT
	rev	CCGCACAACCTTTGGTGTGG
TP53INP	fwd	TTCTCCAACCAAGAACCAGA
	rev	AGTAGGTGACTCTTCACTGATG
TRIB2	fwd	CTCAAGCTGCGGAAATTCAT
	rev	TTGTCCGAGAGGGGAATCATC
TRPS1	fwd	CTTGGCCCTTATAACATGG
	rev	CCTTGGCAATCTGGTGTGTTT
UBE2D3	fwd	CAGGTCCAGTTGGGGATGATA
	rev	AAGAATACACCGCCTTGATATGG

Positive control genes:

E2F1	fwd	TGCCAAGAAGTCCAAGAACC
	rev	CAGCTGTCCGAGGTCCTG
NRAS	fwd	GCTTCCTCTGTGATTTTGCCA
	rev	GCACCATAGGTACATCATCCG

Housekeeping genes (endogenous controls):

ACTB	fwd	AGAGTACGAGCTGCCTGAC
	rev	AGCACTGTGTTGGCGTACAG
LMNB1	fwd	CTGGAATGTTTGCATCGAAGA
	rev	GCCTCCCATTTGGTTGATCC
PGK1	fwd	AAGTGAAGCTCGGAAAGCTTCTAT
	rev	TGGAAAAAGATGCTTCTGGG

Cycling program for qRT-PCR:

Analyses were carried out using the Fast SYBR Green Master Mix (Applied Biosystems) with a 7900HT Fast Real-Time PCR System (Applied Biosystems) in the fast mode:

Step	Temperature (°C)	Duration	
AmpliTaq® Fast DNA Polymerase, UP Activation	95	20 sec	hold
Denaturation	95	5 sec	} 40 cycles
Annealing/extension	60	20 sec	
Measurement (temperature suitable for all primers used)	69	20 sec	
	95	15 sec	hold
Dissociation curve	65	15 sec	(dissociation ramp rate 1% step)
	90	15 sec	

Online Supplementary Table S4. SAM analysis for the identification of *NPM1*^{mut}-associated gene signature.

See attached Excel file: ARUSS_Supplementary Table S4 for the SAM list of significant genes *NPM1*^{mut} versus *NPM1*^{wt}, which was used for further integrative analysis. The 307 genes overlapping between the lists of predicted target genes and the *NPM1*^{mut} associated GEP are highlighted in blue (genes were down-regulated and the putative targeting miRNA was up-regulated).

Online Supplementary Table S5. SAM list of 66 significant miRNAs differentially expressed between *NPM1*^{mut} and *NPM1*^{wt} as determined by BRB Array Tools. The 66 miRNAs were determined by SAM *NPM1*^{mut} versus *NPM1*^{wt}; false discovery rate = 0.09631. The geometric means of ratios (red signal/green signal) in each class and the fold difference of geometric means (*NPM1*^{mut}/*NPM1*^{wt}) are given.

Geom mean of ratios red/green in class 1 : <i>NPM1</i> MUT	Geom mean of ratios red/green in class 2 : <i>NPM1</i> wt	Fold difference of geom means (<i>NPM1</i> MUT / <i>NPM1</i> wt)	name of mature miRNA	Garzon et al., PNAS 2008
2.112	0.867	2.436	hsa-miR-10a	X
1.278	0.793	1.612	hsa-miR-10b	X
0.505	0.246	2.053	hsa-let-7b	
0.498	0.298	1.671	hsa-miR-29a	X
1.555	1.122	1.386	hsa-miR-196b	
0.385	0.167	2.305	hsa-let-7c	X
0.591	0.428	1.381	hsa-miR-30c	
0.070	0.033	2.121	hsa-miR-21	X
0.340	0.159	2.138	hsa-let-7a	X
0.464	0.272	1.706	hsa-miR-20a	X
0.316	0.193	1.637	hsa-miR-23b	
0.867	0.608	1.426	hsa-miR-30b	
0.370	0.234	1.581	hsa-miR-23a	
0.351	0.177	1.983	hsa-let-7d	X
0.341	0.237	1.439	hsa-miR-200b	
0.791	0.625	1.266	hsa-miR-98	X
0.940	0.736	1.277	hsa-miR-19a	X
1.097	0.897	1.223	hsa-miR-373	
0.519	0.334	1.554	hsa-miR-92a	
1.277	1.039	1.229	hsa-miR-199a-3p	
1.269	1.056	1.202	hsa-miR-136	
0.992	0.757	1.310	hsa-miR-29c	X
0.649	0.515	1.260	hsa-miR-491-5p	
0.991	0.809	1.225	hsa-miR-224	
0.725	0.578	1.254	hsa-miR-125a-5p	
0.326	0.198	1.646	hsa-let-7f	X
1.297	1.120	1.158	hsa-miR-369-3p	X
0.309	0.211	1.464	hsa-miR-106a	X
0.382	0.285	1.340	hsa-miR-27b	
0.723	0.585	1.236	hsa-let-7e	
0.414	0.293	1.413	hsa-miR-27a	
1.310	1.138	1.151	hsa-miR-380	
1.468	1.271	1.155	hsa-miR-526b*	
0.938	0.818	1.147	hsa-miR-151-5p	
1.352	1.176	1.150	hsa-miR-518c*	
0.354	0.261	1.356	hsa-miR-17	X
0.823	0.693	1.188	hsa-miR-320	
1.039	0.837	1.241	hsa-miR-155	X
0.572	0.434	1.318	hsa-miR-15a	X
1.039	0.910	1.142	hsa-miR-124	
0.807	0.674	1.197	hsa-miR-493*	
1.115	0.967	1.153	hsa-miR-340*	
0.333	0.218	1.528	hsa-miR-16	X
0.561	0.432	1.299	hsa-miR-19b	X
0.503	0.376	1.338	hsa-miR-15b	
0.613	0.508	1.207	hsa-miR-30a	
1.300	1.173	1.108	hsa-miR-379	
1.052	0.909	1.157	hsa-miR-195	X
0.943	0.831	1.135	hsa-miR-29b	X
0.544	0.477	1.140	hsa-miR-18a	X
0.749	0.659	1.137	hsa-miR-105	
1.224	1.092	1.121	hsa-miR-142-5p	X
0.566	0.460	1.230	hsa-miR-221	
1.212	1.102	1.100	hsa-miR-28-5p	
0.652	0.591	1.103	hsa-miR-494	
0.406	0.359	1.131	hsa-miR-125b	
1.365	1.251	1.091	hsa-miR-381	
1.318	1.202	1.097	hsa-miR-382	
0.649	0.573	1.133	hsa-miR-30e	
0.845	0.777	1.088	hsa-miR-339-5p	
0.718	0.655	1.096	hsa-miR-7	
0.913	0.815	1.120	hsa-miR-361-5p	
1.040	0.805	1.292	hsa-miR-223	
0.545	0.491	1.110	hsa-miR-146a	
0.956	1.149	0.832	hsa-miR-495	
0.606	0.770	0.787	hsa-miR-192	X
overlap				24 miRNAs

miRNAs upregulated in *NPM1*mut

miRNAs downregulated in *NPM1*mut

33 core miRNAs

Online Supplementary Table S6. Overview of qRT-PCR target gene validation results. miRNA-target gene relations (n=42 genes; 177 different miRNA-target gene pairs) were investigated by analyzing target gene mRNA levels by qRT-PCR in HeLa cells transfected with either of one of 11 synthetic miRNA mimics or a negative control RNA. In accordance with previous reports of no significant effects of this particular miRNA on mRNA level, we also found no mRNA level changes for the known miR-19a-CCND1 and miR-155-FOXO3 interaction.¹²⁻¹³

microRNA	let-7a	miR-15a	miR-19a	miR-20a	miR-23a	miR-29a	miR-30c	miR-106a	miR-142-5p	miR-155	miR-369-3p
putative target genes											
ABCC5 (alias: MRP5)	M T P	T P		T	M T		M	T	T		T
AKAP13	P (let-7d)	T		T P		T P	T	T P (106b)			
APP	M	T P		M T P ref. 1	T	M		M T P ref. 2			P
BCL2L1	T P						T				
CCND1	T P	T P ref. 3	T # ref. 4	T P ref. 5	T P			T P (106b)	T	T	T
CLCN3		T + lucif			M T P				T P	T	
CRKL	M (let-7i)	M T P + lucif				T	T P				
DUSP16	T P										
FOXA1				T P	M T P		T P	T P (106b)	T		
FOXO1 (previous: FOXO1A)		T									T P
FOXO3					T	T	T P		T	T # ref. 6	
FOXO4 (previous: MLLT7)					T P	T P					
GAB1				T P		M T P	M (30e) T	M T P (106b)	T		M
GSPT1	M										
ID2			T				M (30e)		T		
IRF2				P + lucif	T P						
ITGA6			T P		T	T P	T P		T		
KAT2B (previous: PCAF)			T P	T P	T			T P (106b)	T		
KIT			T P + lucif	T + lucif				T	T P		
LPP		T	M T P		T		T P		T	T	
LRP6		M T P	M	T		T	T	T			
MAP4K4	T P				T	T	T		T P	T	T
MLL							T		T		T
MN1		T + lucif	T P								
MX11				T		T P		T	T P		
NRP1 (neuropilin 1)						M	T P		T P		
OTX2	P						P		T P		
PAWR							M (30d) T P				T
PIK3CA			M T							M T	
PRKCE	P (let-7d)		T		T	T					T
PROM1 (alias: CD133)					T	M (29b) T	T		T		T
RALA			T			T	P (30a, 30e)				T
SERPINB9 (previous: PI9)	T	T				M T + lucif					T
SIRT1 (sirtuin 1)			T		T	T	T P		T	T	T P
SP100						T	T				
SP140	M										
SPARC (osteonectin)			T	T	T	T P ref. 7 + lucif		T			T
TAL1			T	T P		T		T P (106b)			
TP53INP	T		T P	T P	T	T P	T P	T P (106b)	T P	M T P ref. 8	T
TRIB2	T P					T P					
TRPS1			T P	T P	T		T P	T P		T P	T P
UBE2D3					T		T			T	T

positive control genes (genes not out of signature)

E2F1				T P ref. 9		T		T P ref. 9			
NRAS	T P ref. 10										

housekeeping genes (endogenous controls)

LMNB1 (lamin B1)					T ref. 11		P (30a, 30e)		P		
ACTB (beta actin)			T								
PGK1			T						T		

M T P target prediction algorithm: M = MicroCosm Targets (formerly miRBase Targets); T = TargetScan (Release 5.1); P = PicTar (Lall et al 2006)
= no mRNA reduction described in literature

+ lucif target validated with luciferase reporter assay in this study

Green mRNA reduction more than 30% **Yellow** mRNA reduction 10-30% **Grey** no mRNA reduction **Blue** gene described as target in literature with reference (ref.)

Colors were assigned according to mean expression of the gene (mean of 2 independent transfection and qRT-PCR experiments (measured in duplicates): harvest at 2 different time points, normalization by 3 different housekeeping genes).

References (genes described as targets in literature):

ref. 1: Hébert et al., Neurobiol Dis. 2009 ref. 2: Patel et al., Mol Neurodegener. 2008 ref. 3: Bonci et al., Nat Med. 2008
ref. 4: Qin et al., Proc Natl Acad Sci U S A. 2010 ref. 5: Yu et al., J Cell Biol. 2008 ref. 6: Kong et al., J Biol Chem. 2010
ref. 7: Kapinas et al., J Cell Biochem. 2009 ref. 8: Gironella et al., Proc Natl Acad Sci U S A. 2007
ref. 9: O'Donnell et al., Nature. 2005 ref. 10: Johnson et al., Cell. 2005 ref. 11: Lin and Fu, Dis Model Mech. 2009

For detailed references see Supplementary Information.

References for Online Supplementary Table S6

1. Hebert SS, Horre K, Nicolai L, Bergmans B, Papadopoulou AS, Delacourte A, et al. MicroRNA regulation of Alzheimer's Amyloid precursor protein expression. *Neurobiol Dis.* 2009;33(3):422-8.
2. Patel N, Hoang D, Miller N, Ansaloni S, Huang Q, Rogers JT, et al. MicroRNAs can regulate human APP levels. *Mol Neurodegener.* 2008; 3:10.
3. Bonci D, Coppola V, Musumeci M, Addario A, Giuffrida R, Memeo L, et al. The miR-15a-miR-16-1 cluster controls prostate cancer by targeting multiple oncogenic activities. *Nat Med.* 2008;14(11):1271-7.
4. Qin X, Wang X, Wang Y, Tang Z, Cui Q, Xi J, et al. MicroRNA-19a mediates the suppressive effect of laminar flow on cyclin D1 expression in human umbilical vein endothelial cells. *Proc Natl Acad Sci USA.* 2010;107(7):3240-4.
5. Yu Z, Wang C, Wang M, Li Z, Casimiro MC, Liu M, et al. A cyclin D1/microRNA 17/20 regulatory feedback loop in control of breast cancer cell proliferation. *J Cell Biol.* 2008;182(3):509-17.
6. Kong W, He L, Coppola M, Guo J, Esposito NN, Coppola D, et al. MicroRNA-155 regulates cell survival, growth, and chemosensitivity by targeting FOXO3a in breast cancer. *J Biol Chem.* 2010;285(23):17869-79.
7. Kapinas K, Kessler CB, Delany AM. miR-29 suppression of osteonectin in osteoblasts: regulation during differentiation and by canonical Wnt signaling. *J Cell Biochem.* 2009;108(1):216-24.
8. Gironella M, Seux M, Xie MJ, Cano C, Tomasini R, Gommeaux J, et al. Tumor protein 53-induced nuclear protein 1 expression is repressed by miR-155, and its restoration inhibits pancreatic tumor development. *Proc Natl Acad Sci USA.* 2007;104(41):16170-5.
9. O'Donnell KA, Wentzel EA, Zeller KI, Dang CV, Mendell JT. c-Myc-regulated microRNAs modulate E2F1 expression. *Nature.* 2005;435(7043):839-43.
10. Johnson SM, Grosshans H, Shingara J, Byrom M, Jarvis R, Cheng A, et al. RAS is regulated by the let-7 microRNA family. *Cell.* 2005;120(5):635-47.
11. Lin ST, Fu YH. miR-23 regulation of lamin B1 is crucial for oligodendrocyte development and myelination. *Dis Model Mech.* 2009;2(3-4):178-88.
12. Qin X, Wang X, Wang Y, Tang Z, Cui Q, Xi J, et al. MicroRNA-19a mediates the suppressive effect of laminar flow on cyclin D1 expression in human umbilical vein endothelial cells. *Proc Natl Acad Sci USA.* 2010;107(7):3240-4.
13. Kong W, He L, Coppola M, Guo J, Esposito NN, Coppola D, et al. MicroRNA-155 regulates cell survival, growth, and chemosensitivity by targeting FOXO3a in breast cancer. *J Biol Chem.* 2010;285(23):17869-79.

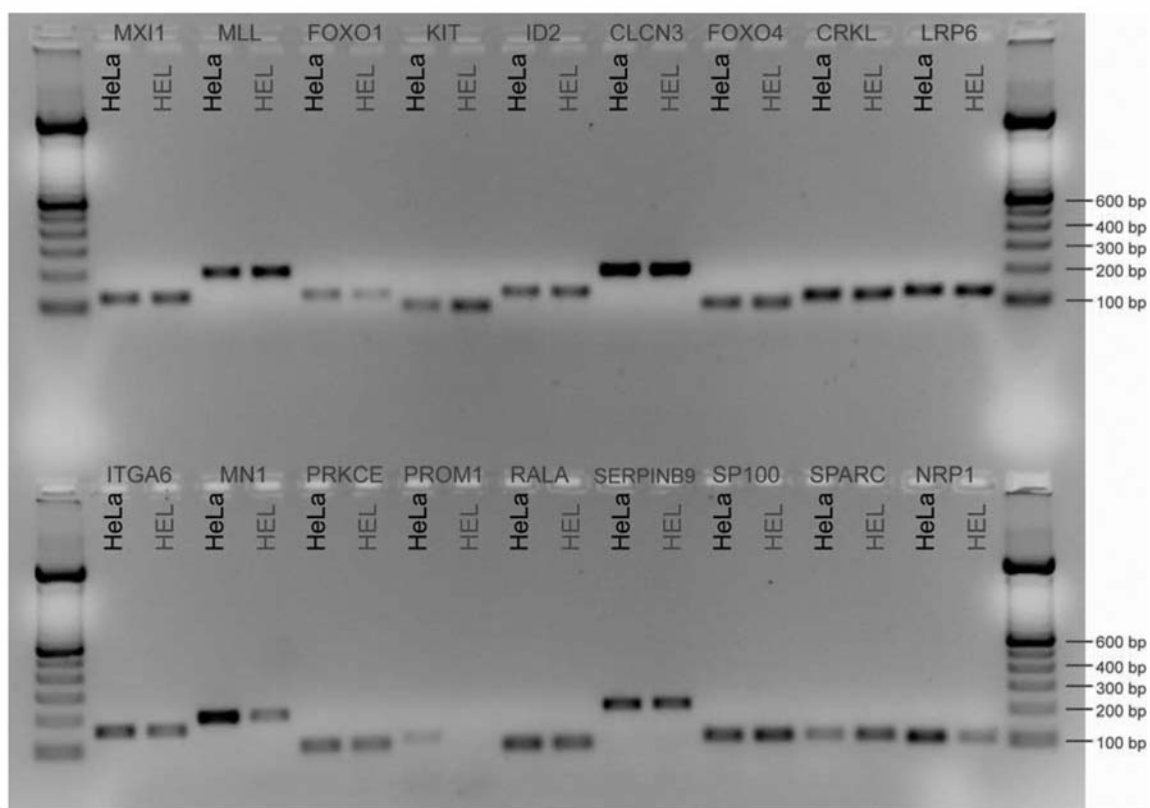
Online Supplementary Table S7. *NPM1*^{mut}-associated, downregulated genes and core miRNAs predicted to target the respective genes.

See attached Excel file: [ARuss_Supplem Table S7](#)

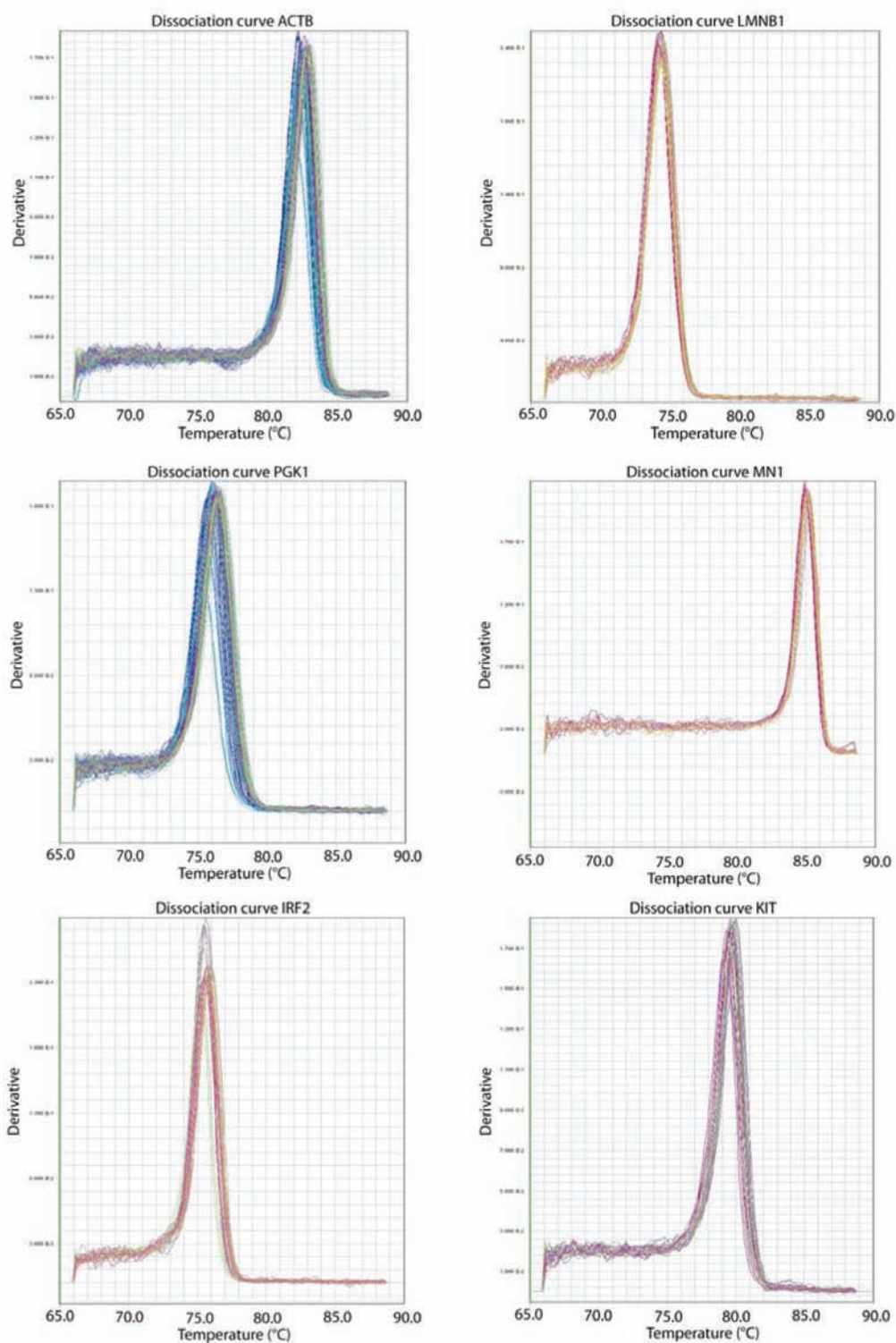
Online Supplementary Table S8. Validation of predicted miRNA targets by qRT-PCR. Normalized qRT-PCR analyses of selected miRNA target genes in HeLa cells which were transfected with the indicated miRNA mimic or negative control and harvested 24 or 48 h post-transfection. The values of normalization by three different housekeeping genes, as depicted in Figure 3 in the main manuscript, are given. The values given are the mean values of two independent transfections and qRT-PCR experiments.

	normalization by		
	ACTB	LMNB1	PGK1
SPARC_29a_24h	0.59	0.88	0.51
SPARC_29a_48h	0.42	0.57	0.43
SPARC_23a_24h	0.87	1.61	0.87
SPARC_23a_48h	0.63	0.99	0.70
CCND1_15a_24h	0.61	0.66	0.52
CCND1_15a_48h	0.81	1.00	0.69
CCND1_20a_24h	0.69	0.55	0.58
CCND1_20a_48h	0.97	0.94	0.83
CCND1_let-7a_24h	0.81	0.80	0.82
CCND1_let-7a_48h	0.79	0.63	0.59
CCND1_106a_24h	0.44	0.49	0.51
CCND1_106a_48h	0.65	0.73	0.69
CCND1_142-5p_24h	0.72	0.68	0.76
CCND1_142-5p_48h	0.83	0.76	0.81
CCND1_155_24h	0.69	0.66	0.92
CCND1_155_48h	0.57	0.58	0.59
CRKL_15a_24h	0.65	0.71	0.62
CRKL_15a_48h	0.61	0.75	0.59
CRKL_30c_24h	0.89	0.73	0.90
CRKL_30c_48h	0.70	0.66	0.84
IRF2_20a_24h	0.67	0.72	0.61
IRF2_20a_48h	0.56	0.74	0.58
IRF2_23a_24h	0.58	1.07	0.58
IRF2_23a_48h	0.61	0.95	0.67
KIT_19a_24h	0.55	0.50	0.55
KIT_19a_48h	0.25	0.30	0.32
KIT_20a_24h	0.51	0.57	0.47
KIT_20a_48h	0.46	0.64	0.51
MN1_15a_24h	0.59	0.64	0.58
MN1_15a_48h	0.73	0.90	0.70
SERPINB9_let-7a_24h	0.52	0.46	0.44
SERPINB9_let-7a_48h	0.63	0.57	0.43
SERPINB9_29a_24h	0.36	0.56	0.32
SERPINB9_29a_48h	0.26	0.37	0.27
SERPINB9_369-3p_24h	1.17	1.12	1.10
SERPINB9_369-3p_48h	0.55	0.55	0.75

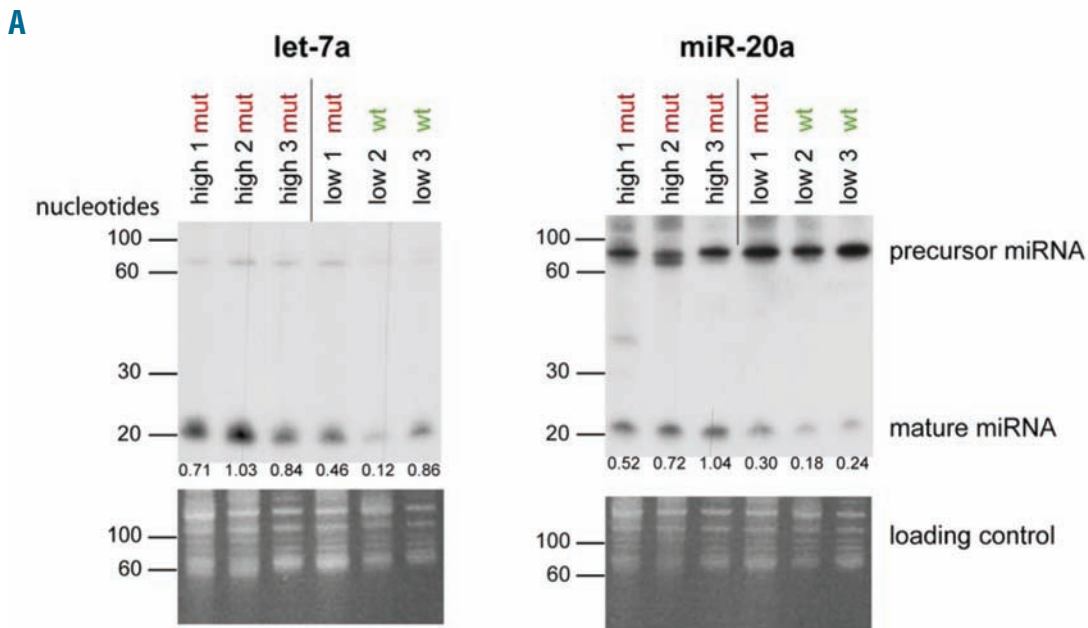
Online Supplementary Figure S1. Agarose gel picture of primer testing by conventional PCR. Prior to qRT-PCR, all primers were tested for sensitivity and specificity by conventional PCR using HeLa and HEL cDNA. The annealing temperature was 60 °C. Only primers resulting in one amplicon of the correct size were included in further analyses. Exemplary amplicons are shown below.



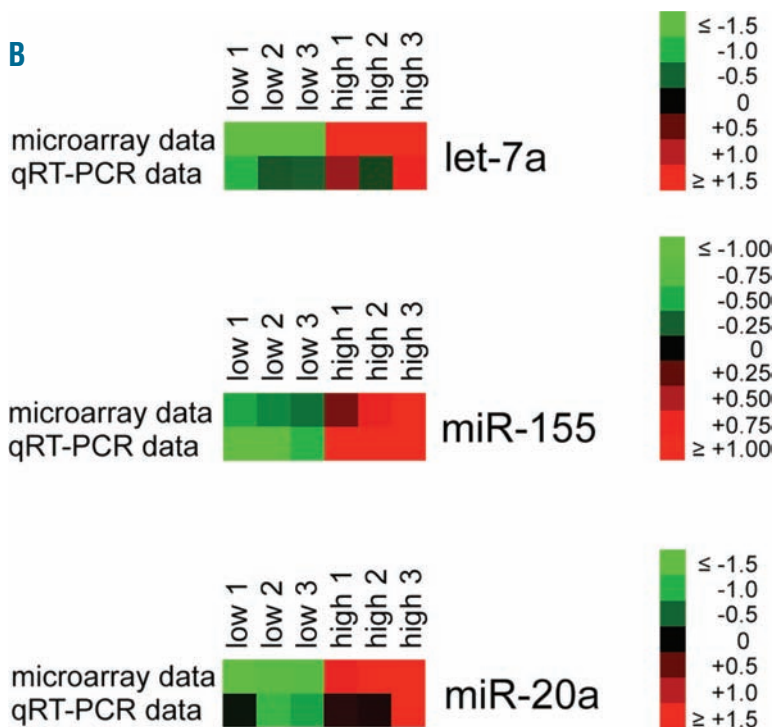
Online Supplementary Figure S2. Dissociation curve graphs (qRT-PCR) of exemplary amplicons. All primers were tested for sensitivity and specificity by conventional PCR and qRT-PCR (annealing temperature 60 °C), resulting in one amplicon and one clear peak in the dissociation curve. Dissociation curves of exemplary amplicons are shown for the three housekeeping genes *ACTB*, *LMNB1* and *PGK1* as well as of investigated target genes *MN1*, *IRF2* and *KIT*.



Online Supplementary Figure S3A. Validation of miRNA microarray results by miRNA northern blot analysis. For northern blot analyses, 10 μ g of total RNA were loaded. RNA originated from the same isolation as the sample previously hybridized to the microarray. "High" and "low" refer to expression of the miRNA on the array. mut = *NPM1* mutated; wt = *NPM1* wild-type. Upper panels: autoradiography films; lower panels: loading control, ethidium bromide stained gels. The numbers given show quantitation of mature miRNA bands, normalized by loading control (the sum of all bands was used). Quantitation was performed with ImageJ (available at <http://rsbweb.nih.gov/ij/>).

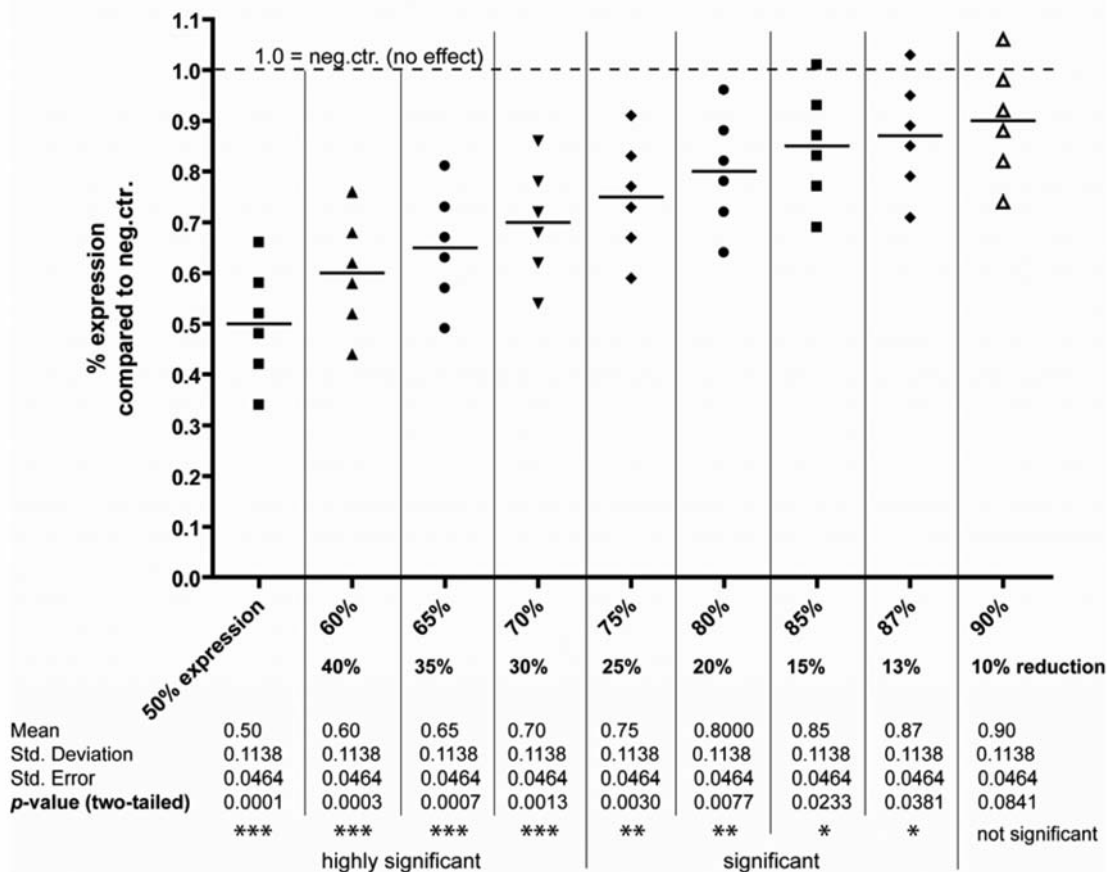


Online Supplementary Figure S3B. Validation of miRNA microarray results by miRNA qRT-PCR analysis. Three patients' samples with either high or low expression of the respective miRNA according to the microarray were analyzed by TaqMan based qRT-PCR (Applied Biosystems). qRT-PCR data were normalized by expression of miR-374, which in the microarray was expressed at a well detectable level with only slight variation among the samples. Heatmaps: \log_2 transformed, mean-centered microarray and corresponding qRT-PCR data (transformed in the same way) are shown. Array data are sorted (low to high) in the plots. Green color = low expression; red color = high expression of the miRNA. Expression data are depicted by color scales, as indicated. Correlation coefficients were as follows: let7a: 0.83; miR-155: 0.82; miR-20a: 0.79. For let-7a, patients "low 1" and "low 3" have wild-type *NPM1*, whereas patients "high 1" and "high 3" have mutated *NPM1*. Normalized, untransformed let-7a qRT-PCR expression data were as follows: "low 1" = 0.57 and "low 3" = 0.84 (mean 0.705), and "high 1" = 2.00 and "high 3" = 3.01 (mean 2.505). This results in a ratio "high 3" / "low 1" = 5.28, and a mean ratio $NPM1^{mut} / NPM1^{wt}$ = 3.55. [Note: Patient "low2" had a t(8;21) and patient "high2" a t(11q23), as these patients were part of an originally larger cohort of 91 AML cases including all cytogenetic subgroups.]

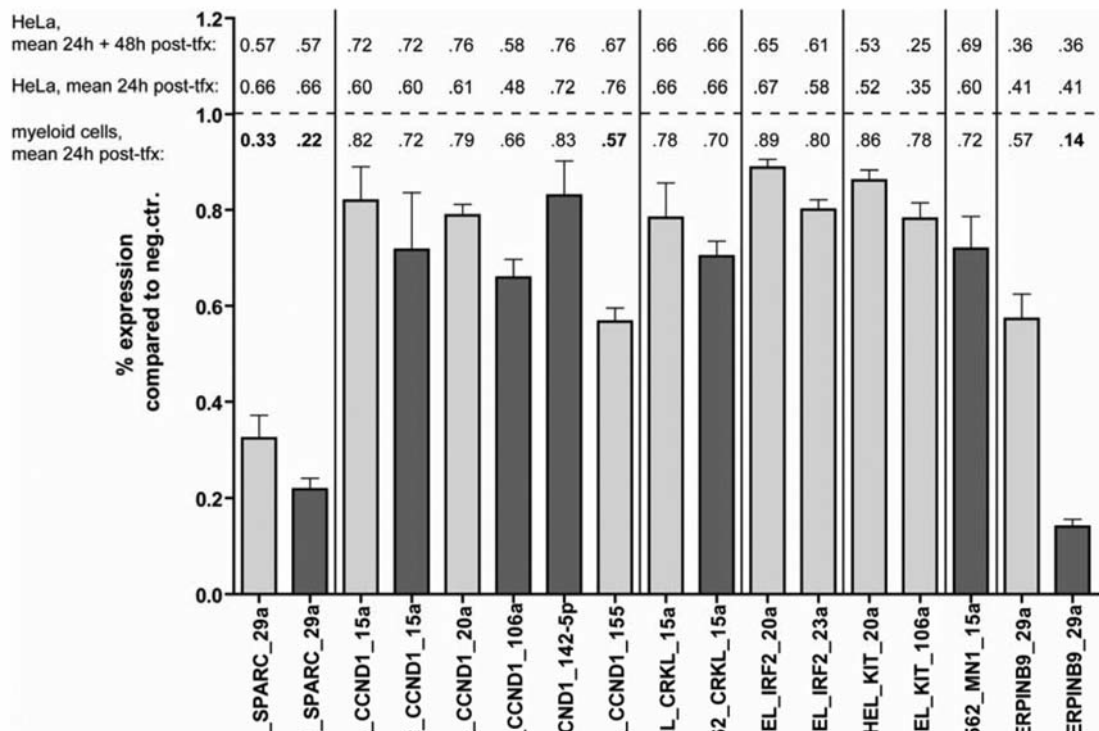


Online Supplementary Figure S4. Hypothetical expression values to determine the significance levels of qRT-PCR data (as depicted in *Online Supplementary Table S6* and Figure 3). Hypothetical normalized expression values compared to the negative control, which is set to 1 are shown. The six data points of each reduction stage show the same standard deviation of 0.1138, which is the average standard deviation of the qRT-PCR data shown in Figure 3 (for the genes depicted in Figure 3, the average standard deviation for the six data points was 0.118, as seen for example for CCND1-miR-106a or MN1-miR-15a). The expression cut-offs underlying the color coding of *Online Supplementary Table S6* (dark green: >30% reduction of mRNA compared to negative control transfected cells, and yellow: 10-30% reduction) are based on the significance levels, as shown in the table below. In general, a reduction of mRNA of more than 30% results in highly significant *P* values ($P < 0.001$; one-sample *t* test, compared to 1.0 = negative control), whereas a 10-30% reduction with average SD results in significant *P* values ($P = 0.001 - 0.05$).

hypothetical expression values
50-90% expression compared to neg.ctr.
SD 0.1138



5online Supplementary Figure S5. Validation of predicted miRNA targets by qRT-PCR in myeloid cells and comparison to effects observed in HeLa cells. Selected miRNA-target gene interactions were validated in two myeloid cell lines (HEL, transfected with miR-15a, -20a, -23a, -29a, -106a and miR-155; K-562, transfected with miR-15a, -29a, -106a and miR-142-5p). While these suspension cells displayed poorer transfectability than HeLa cells (see *Online Supplementary Design and Methods*), we nevertheless could reproduce all previous findings in these cell lines (the relations *CCND1*-miR-106a and *MN1*-miR-15a were seen in K-562 cells only), although with a lower but consistent reduction of target mRNA levels. Of note, transfection of K-562 cells (dark gray bars) resulted in greater effects as compared to HEL cells (light gray bars), which was possibly due to the higher transfection efficiency observed for K-562 cells (K-562: 68% of total cells; HEL: 58%). Interestingly, the effects of miR-29a transfection on target mRNA levels of *SPARC* were higher in both myeloid cell lines and for *SERPIN9* higher in K-562 cells compared to HeLa cells. Normalized qRT-PCR results of selected miRNA target genes in HEL and K-562 cells which were transfected with the indicated miRNA mimic or negative control and harvested 24 h post-transfection are depicted. Each bar represents the mean effect plus standard deviation by normalization with the housekeeping genes *ACTB* and *PGK1* of two independent transfection and qRT-PCR experiments. Each value is calculated as percentage expression of target gene mRNA of miRNA-of-interest transfected cells compared to negative control (1.0 = 100%) transfected cells.



Online Supplementary Figure S6. Validation of miRNA targets by luciferase reporter experiments. Modified presentation of data contained in Figures 4C and 4D. Here, only the first column (reporter construct with wt binding site and co-transfection of negative control RNA) of each miRNA-target gene pair analyzed was set to 1 and the other conditions were set in relation to it. Differences in basal luciferase expression levels might be due to formation of different secondary structures of RNA of the reporter constructs with wild-type or mutant binding sites. Variations in plasmid DNA preparations should also be taken into account. (C) and (D) Normalized ratios firefly/renilla luciferase as determined by reporter assays in HeLa cells which were transfected with the indicated miRNA mimics or a negative control (neg.ctr. and wt construct; ratio set to 1) and co-transfected with the pMIR-REPORT vector containing the 3'UTR of candidate target genes downstream of the firefly luciferase reporter gene. (C) 3'UTRs containing one putative miRNA binding site, (D) 3'UTRs containing two putative miRNA binding sites. MiRNA binding sites were either wild-type (wt; dark gray bars) or mutated (mut 1BS = 1 binding site mutated, mut 2BS = both binding sites mutated; light gray bars). Bars represent the mean of two independent experiments with transfections performed in triplicate, error bars depict the standard deviation (SD). All effects observed were highly significant ($P < 0.001$; unpaired t test).

